Available online at www.sciencedirect.com
ScienceDirect
Journal of the European Ceramic Society 30 (2010) 1619–1627
www.elsevier.com/locate/jeurceramsoc

Influence of scrap glass powders and the maturing process in the unfired state on the body properties of a kaolinitic clay after firing

Anja Schwarz-Tatarin [a,*], Sabine Freyburg [b]

[a] *Hans Lingl Anlagenbau und Verfahrenstechnik GmbH & Co. KG, Nordstraße 2, 86381 Krumbach, Office Weimar, Germany*
[b] *F.A. Finger-Institute for Building Materials Science, Bauhaus-University Weimar, Coudraystraße 11a, 99423 Weimar, Germany*

Received 27 June 2009; received in revised form 29 December 2009; accepted 10 January 2010
Available online 1 February 2010

Abstract

For the ceramic and brick industry as an energy-intensive sector solutions to diminish the energy consumption are of crucial importance. One possibility to affect the energy consumption of the firing process is the use of sintering aids, e.g. secondary raw materials like scrap glass powders.

The knowledge of the mineral and liquid phase formation during firing is a basic requirement to assess the physical properties of the fired body. The impact of the scrap glass powders depends to a great extent on the respective clay composition, but also on both the chemical composition and the degree of preparation of the glass. The present paper discusses phase formations during firing and the resulting body properties, both of which depend significantly on interactions between clay and glass during maturation. A material model for describing the mode of action of scrap glass powders within kaolinitic clays is presented.

Keywords: Sintering; X-ray methods; Traditional ceramics; Structural applications; Phase reactions

1. Introduction and theoretical background

For the ceramic and brick industry as an energy-intensive sector solutions to diminish the energy consumption are of crucial importance. In the forthcoming decades increasing production costs are to be due to increasing energy costs and decreasing amounts of fossil fuels. Furthermore, the use of natural resources is inevitably connected with environmental changes and hence with additional costs, e.g. for the renaturation of disused clay deposits. Moreover, in other industries by-products accrue which are not used so far and hence have to be deposited.

An alternative application of such secondary raw materials is their use in silicate ceramic bodies. The impact of secondary raw materials on the physical properties of the fired body had already been systematised by earlier investigations.[1] However, the knowledge of the mineral and liquid phase formation during firing is a basic requirement to apply secondary raw materials in ceramic bodies in a technically and economically advantageous way. The present paper emerged from a series of investigations for which four clays and five scrap glass powders different in mineralogy, chemistry and particle size distribution had been used. The overriding aim of these investigations was to clarify the mode of action of scrap glass powders in silicate ceramic bodies with regard to the whole production process. This paper excerpts investigations and results of the phase formations during firing and resulting body properties which significantly depend on interactions between clay and glass during maturation.

There are complex phase reactions occurring during firing of silicate ceramic bodies due to the large number of mineral phases clays consist of. With regard to the phase reactions, mainly bodies rich and poor in earth alkalis, respectively, are distinguished.[2–4] In consideration of the microstructures formed during firing Freyburg[5] classified four types of clays by which the durability of the respective bodies can be assessed. Due to the strongly varying composition of natural silicate raw materials occurring phase reactions can merely be estimated. The presence of further minerals or impurities leads to changed phase reactions during firing. In the following, the basic knowledge of phase formations and transitions will be described.

During firing of kaolinitic clays mullite formation takes place even under the presence of further compounds (Fig. 1).

* Corresponding author. Tel.: +49 3643 494830; fax: +49 3643 494898.
E-mail address: a.schwarz-tatarin@lingl.com (A. Schwarz-Tatarin).

0955-2219/$ – see front matter © 2010 Elsevier Ltd. All rights reserved.
doi:10.1016/j.jeurceramsoc.2010.01.015

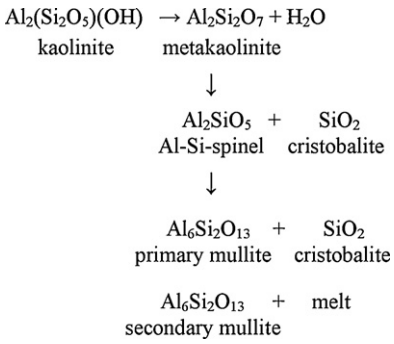

Fig. 1. Schematic of the kaolinite transformation during firing.

Furthermore, depending on the composition of the raw material batch the formation of cristobalite and spinel is possible. After the dehydroxylation of the clay minerals the formation of primary mullite from clay mineral metaphases and the segregation of cristobalite without liquid phases take place. Thereby, the activation energy for mullite nucleation and mullite growth depends on the defective structure of the starting kaolinite.[6,7] After Sadunas et al.[8] the intensity of mullite formation is strongly relating to the presence of bivalent metal ions and decreases in the order $Cu^{2+} > Fe^{2+} > Mn^{2+} > Co^{2+} > Ni^{2+} > Cr^{2+}$. The formation of primary mullite at 900–1000 °C is a solid state reaction. Not till higher temperatures SiO_2 is segregated as silica as a liquid phase.[4,5,9,10,11]

2. Experimental

For the investigations natural clays and industrial secondary raw materials were used. Such raw materials are applied within the ceramic industry, e.g. to produce facing and clinker bricks, vertically perforated bricks or roofing tiles.

Since, they are many component systems consisting of a large number of clay and non-clay minerals which influence each other during processing, investigations on model systems consisting of comparatively pure materials like kaoline give no practicable results. The clay used for the investigations had been selected according to the microstructure-oriented clay classification after Freyburg[5] and represents a typical natural clay used for production of clinker bricks. All characteristics of this clay A are shown in Tables 1 and 2.

Table 2
Cation exchange capacity and granulometrical parameters of clay A.

Cation exchange capacity	
CEC [meq/100 g]	12
Specific surface area [m²/g]	
BLAINE [m²/g]	0.73
BET [m²/g]	49.74
Particle size distribution	
Medium gra in size xm [μm]	1.44
Mostly contained grain size x_{modal} [μm]	0.57
Grain size at 50% pass x50 [μm]	0.63

The mineralogical composition had been determined by X-ray diffraction of oriented clay mineral preparations according to the classic method[12]. Data had been collected by an X-ray powder diffractometer D 5000 (Siemens, Germany) in Bragg–Brentano geometry (operation modes: Cu-Kα radiation, $\lambda \approx 0.154$ nm, 4–60° 2θ range, 0.05° step size, 2.5 s step time). The cation exchange capacity (CEC) had been determined by exchange of copper(II)-triethylenetetramine after Meier and Kahr.[13]

For the determination of the specific outer surface area a Blaine analyser Blaine-Star-ZEB-2002-B (Wasagchemie, Sythen GmbH, D) had been used. The density required for this measurement had been determined by pycnometer AccuPyc 1330 (Micromeritics GmbH, Mönchengladbach, D). The determination of the specific inner surface area was carried out after Brunauer, Emmett and Teller (BET) by using an ASAP 2000 (Micromeritics, Mönchengladbach, D).

The grain size distribution was determined by laser diffraction analysis using a Coulter LS 230 (Coulter Cooperation Miami, USA) over a measurement range of 0.04–2000 μm. In order to prevent agglomeration before and during measuring the samples had been ultrasonic-dispersed (2–6 min).

Furthermore, for the investigations four scrap glass powders were used. All characteristics of the glasses are shown in Table 3.

The glass powders G1 and G2 are recycling glasses from a container glass and a flat glass, respectively. The recycling rate

Table 1
Mineralogical, chemical composition and water soluble ions of clay A.

Mineralogical composition [%]

Quartz	Feldspar	Ferreous minerals	Calcite/dolomite	Kaolinite	Muscovite	Illitic mixed-layer minerals + smectite
7	2	1	0	72	5	13

Chemical composition [wt.%]

SiO_2	Al_2O_3	Fe_2O_3	CaO	MgO	TiO_2	K_2O	Na_2O	SO_3	P_2O_5
55.27	36.7	3.26	0.2	0.23	2.55	1.5	0.12	0.01	0.15

Water soluble ions [mmol/l]

Cl	S	N	Ca	Mg	K	Na	pH-value
0.01	0.03	0.00	0.04	0.02	0.02	0.01	6.3

Table 3
Characteristics of the scrap glass powders used.

	G1	G2	G3.1	G3.3	G3.4	G4
Mineralogical composition [%]						
Quartz						2
Amorphous content	100	100	100	100	100	98
Chemical composition [wt.%]						
SiO_2	69.71	69.65	61.00	61.00	61.00	70.39
Al_2O_3	1.96	0.77	16.00	16.00	16.00	1.93
Fe_2O_3	0.51	0.00				1.59
CaO	10.93	10.37	8.00	8.00	8.00	9.00
MgO	0.85	1.73	3.00	3.00	3.00	3.21
MnO		0.32				
TiO_2	0.11	0.07				
K_2O	1.05	0.38				0.30
Na_2O	14.86	16.24				11.59
SO_3		0.28				
B_2O_3			8.00	8.00	8.00	
P_2O_5	0.02	0.21				
BaO			4.00	4.00	4.00	
Content of organic compounds [wt.%]						
Weight loss at 300 °C (STA)						1.04
Water soluble ions [mmol/l]						
Cl		0.01				0.01
S	0.01	0.01		0.03	0.01	0.04
N	0.06	0.06				
Ca	0.06	0.10	0.06	0.09	0.06	0.16
Mg	0.01	0.04	0.02	0.21	0.17	0.07
K	0.01	0.01		0.02		0.01
Na	0.19	0.24		0.01	0.01	1.42
P						0.01
pH-value	10.0	10.0	7.7	10.2	10.0	10.1
Specific surface area [m^2/g]						
BLAINE [m^2/g]	0.32	0.28	0.08	1.24	0.95	0.71
BET [m^2/g]	0.60	0.47	0.12	3.34	2.30	2.88
Particle size distribution						
Medium grain size *x*m [μm]	22.6	32.5	248.9	3.9	5.5	8.3
Mostly contained grain size *x*modal [μm]	41.7	45.8	203.5	2.3	7.1	7.8
Grain size at 50% pass *x*50 [μm]	17.2	24.1	181.8	2.5	3.8	5.6

of such glasses averaged out at 83.6% in the year 2006 and is declining since 2004.[14]

The alkali free borosilicate glass G3 used for the investigations accrues as cullet during the recycling of borofloat glass. It was chosen for the investigations since its chemical composition is completely different to that of the glass powders G1 and G2.

Additionally, the borosilicate glass was further dry milled by MaxxMill R02 Maxx (Maschinenfabrik Gustav Eirich, Germany) using a high yield austenitic steel milling vessel as well as corundum milling balls with a diameter of 4–5 mm. By the variation of the amount of mill material two grades of preparation were gained. The finest glass powder is named G3-3 and the coarser one G3-4, respectively.

The glass powder G4 was obtained by drying a grinding slurry accruing from flat glass processing with a moisture content between 10 wt.% and 30 wt.% and with an amount of 500–700 t/a (at the supplier).

Some of the starting raw materials were existent prepared and some were available in lumpy condition. Initially, the last were crushed and milled to a maximum grain size of 2 mm. Previously, those raw materials accruing as slurry had been dried at 40 °C to a constant mass. For crushing and milling jaw crushers for maximum starting grain sizes of 150 mm and 40 mm, respectively as well as a baffle mill for a maximum starting grain size of 10 mm combined with a 2 mm mesh were used.

In order to investigate the body properties batches and specimens had been prepared as follows.

The dried clay and scrap glass powders were blended and homogenised in the following compositions:

100% clay
90% clay/10% glass (all glass qualities)
75% clay/25% glass (G1 and G2)
70% clay/30% glass (all glass qualities)
50% clay/50% glass (all glass qualities)

Afterwards, the mixtures were blended with deionised water to obtain plastic and extrudable batches. These had been matured for 3–5 days and then extruded by a laboratory extruder with-

out vacuum (Netzsch, Germany) to prism-shaped specimens of 2.5 cm × 1.0 cm × 12.0 cm in size.

The drying was initially carried out at room temperature and afterwards at 100 °C within a laboratory drying chamber UT 20 (Heraeus Instruments, Germany) to a constant mass. Firing was conducted within a laboratory gradient furnace SO 498 (Linn Elektrotherm, Germany) with a heating rate of 2 K/min (1 h soaking time, free cooling down). There were temperature steps of 10 K between two specimens of each composition. Depending on the batch composition firing temperatures between 700 °C and 1200 °C were applied.

The mineralogical composition of the fired samples was determined by X-ray powder diffraction. Initially, the samples were gently milled by a mortar mill RM 100 (Retsch, Germany) and afterwards ground by mortar to a maximum particle size of 40 μm. Data had been collected by an X-ray powder diffractometer D 5000 (Siemens, Germany) in Bragg–Brentano geometry (operation modes: Cu-Kα radiation, $\lambda \approx 0.154$ nm, 4–60° 2θ range, 0.018° step size, 4 s step time).

In order to determine the amorphous content of the bodies the samples had been blended with an internal standard of 20 wt.% CaF_2 and afterwards measured again. The quantitative analysis of the mineral and amorphous phase contents was carried out by Rietveld analysis using the software Topas R V3.0 (Bruker AXS, Germany). For every firing series (one composition fired at different temperatures) the refinement started with all possible phases within the investigated temperature range and eliminated those phases not present in the particular sample. In all samples refinement involved correction of preferred orientation.

The optical assessment of the microstructure was conducted by scanning electron microscopy (SEM S 2700 LB, Hitachi, Japan; high vacuum, acceleration voltage 15 kV). Additionally, chemical composition of single phases was analysed by means of an energy dispersive X-ray detector (EDS TRACOR Voyager 2100, Noran Instruments, USA). The samples had been embedded in resin and polished by diamond paste. In order to obtain a conducting surface, samples had been coated with a gold layer of about 5 nm.

3. Results and discussion

3.1. Unfired state

Investigations on clays and glass powders in the unfired state revealed that the used glass powders are susceptible to dissolution (Fig. 2) due to the high grade of fineness and hence large

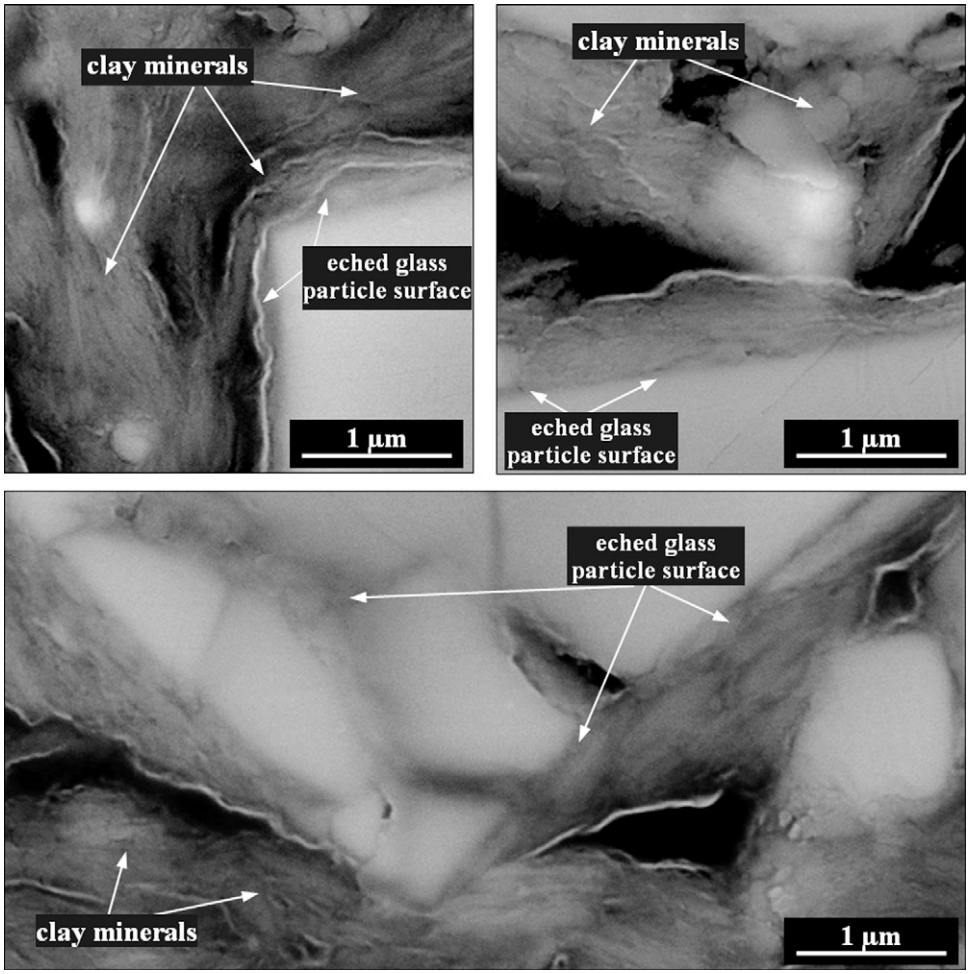

Fig. 2. Microstructure due to particle interactions between clay mineral- and glass surfaces at the unfired state (A + G4, 1:1, water content 45 wt.%; after 5d; ESEM-FEG, high vacuum mode, BSE, 15 kV).

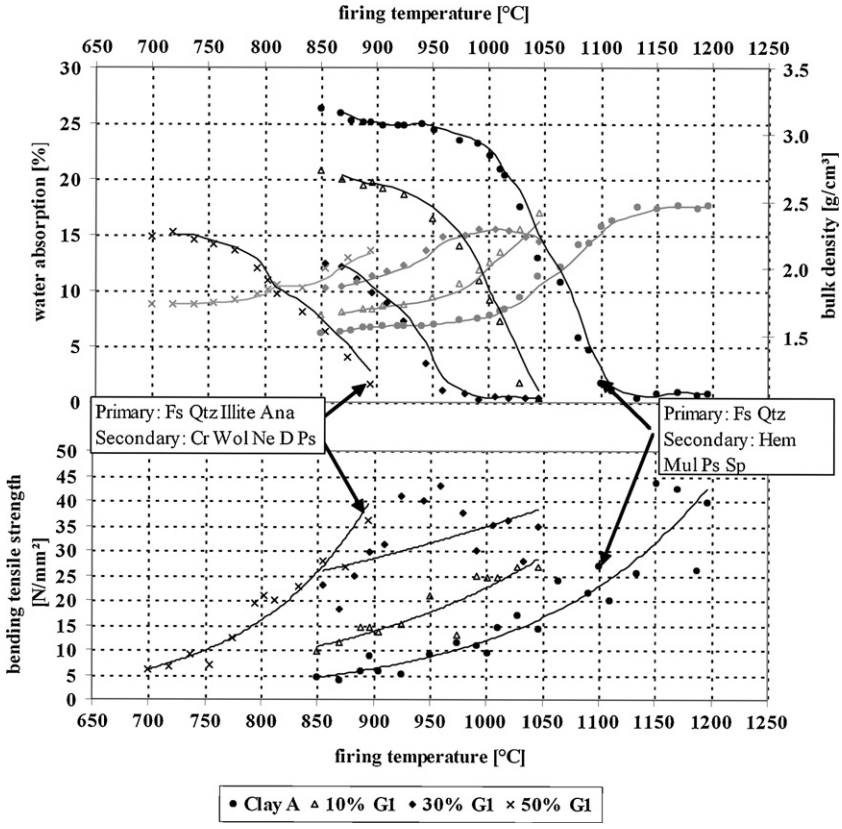

Fig. 3. Development of body properties with different amounts of G1 (gradient firing: ΔT 200 K, heating rate 2 K/min).

specific surface area as well as due to certain predeterioration by milling and grinding processes. Glass dissolution already occurs due to the presence of water and leads to the solution of easily soluble alkalis and earth alkalis from the glass network as well as to an increase in pH-value. In contrast, the addition of alkali free borosilicate glass results in a mainly grogging impact independent from the grade of fineness due to an impeded glass disintegration by high values of Al_2O_3.[15,16]

3.2. After firing

Basically, the addition of scrap glass powders leads to a higher diversity in mineral phases of the body and to lower sintering temperatures. Thereby, the chemical and granulometrical composition of the glass powders strongly influence phase formation. The densely sintered body of the kaolinitic clay A is mainly characterised by formation of mullite, spinel and amorphous phases (Fig. 3). Between 800 °C and 900 °C, due to the alkali containing glass powders G1, G2 and G4 cristobalite, wollastonite, diopside and nepheline are formed. The use of the alkali containing glass powder G4 additionally resulted in the formation of enstatite and in an epidote-similar phase not clearly identified, but most of all fitting the structure of epidote (Table 4). In contrast, the addition of alkali free alumoboro silicate glass merely leads to the formation of cristobalite (G3-1) and akermanite (G3-3), respectively.

Furthermore, in the at 900 °C densely sintered bodies containing 50 wt.% of the glass powders G1, G2 and G4 (alkali containing) primary clay minerals (in this case illite) were detected (Figs. 3 and 4). Moreover, mullite and spinel which indicate sintering of the clay A without glass powder were not present at this firing temperature (Fig. 3). Hence, it can be inferred that sintering of kaolinitic bodies due to alkali containing glasses proceeds without any participation of the clay matrix and is solely initialise by the glass melt. This can explain why, e.g. illite and cristobalite coexist in the same sample.

Furthermore, XRD results (Fig. 4) pointed out that kind and amount of formed phases correlate with the chemical composition and the grade of fineness of the glass powders. At the same firing temperature, the amount of crystalline phases is increased and the amount of amorphous phases is lowered with a higher grade of fineness.

This can be explained by a shifting of formation of liquid phases as well as nucleation and crystallisation to lower temperatures due to the larger specific surface area. Between 800 °C and 900 °C the amounts of amorphous phases decrease with increasing firing temperatures within the glass powder batches of clay A (Figs. 4–6). Since there is no mullite formation, that means that there is no segregation of a crystalline phase from amorphous clay mineral metaphases (metakaolinite), the formation of secondary phases by crystallisation from the melt is proved. A further indicator for the presence of liquid phases is the decreasing amount of quartz with increasing firing temperatures that had been determined already at temperatures between 800 °C and 900 °C for the batches containing G1, G2 and G4. Since merely the glass particles form liquid phases it is

Table 4
Phase formations in clay A without and with alkali containing glass powders G1, G2 and G4 as well as alkali free glass powders G3-1, G3-4 and G3-3 depending on the respective fineness and the firing temperature at which the bodies are densely sintered.

	Without glass (>1100 °C)	Increasing glass fineness				Increasing glass fineness	
		x_m = 32.5 µm G2 (900 °C)	x_m = 22.6 µm G1 (900 °C)	x_m = 8.3 µm) G4 (900 °C)	x_m = 248.9 µm G3-1 (1100 °C)	x_m = 5.5 µm G3-4 (1050 °C)	x_m = 3.9 µm G3-3 (1050 °C)
Clay A	Hem Mul Sp Ps	Hem Ps Cr Wol Ne D	Hem Ps Cr Wol Ne D	Hem Ps Cr Wol Ne D En Ep	Hem Mul Sp Cr	Hem Mul	Hem Mul Ak

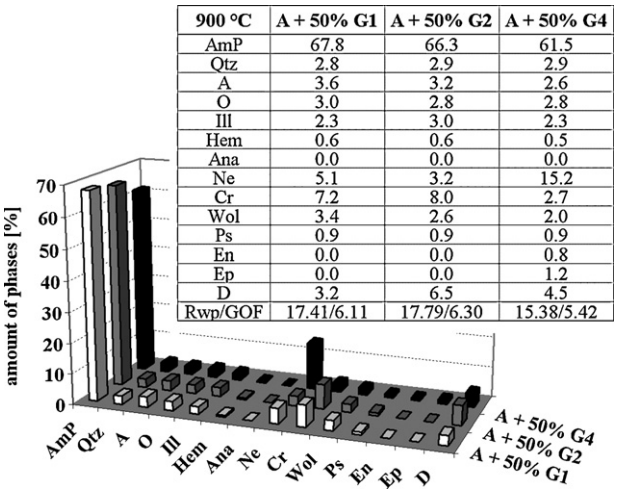

900 °C	A + 50% G1	A + 50% G2	A + 50% G4
AmP	67.8	66.3	61.5
Qtz	2.8	2.9	2.9
A	3.6	3.2	2.6
O	3.0	2.8	2.8
Ill	2.3	3.0	2.3
Hem	0.6	0.6	0.5
Ana	0.0	0.0	0.0
Ne	5.1	3.2	15.2
Cr	7.2	8.0	2.7
Wol	3.4	2.6	2.0
Ps	0.9	0.9	0.9
En	0.0	0.0	0.8
Ep	0.0	0.0	1.2
D	3.2	6.5	4.5
Rwp/GOF	17.41/6.11	17.79/6.30	15.38/5.42

Fig. 4. Amounts of crystalline and amorphous phases due to alkali containing scrap glass powders in clay A (mix ratios 1:1; firing temp. 900 °C, heating rate 2 K/min; XRD/Rietveld, standard: 20 wt.% CaF_2, refinement steps: preferred orientation (*h k l*): Qtz (0 1 0), Ill (1 −1 −1), Wol (0 0 2)).

inferred that quartz melting starts at the quartz–glass interface (Fig. 7).

Furthermore, microstructure observation by SEM proves that wollastonite solely crystallises at the regions of glass particles and in the form of long needles (Fig. 8). The crystals seem to start growth from defective glass regions that is the glass particle rim as well as cracks which had already been formed in the unfired state (Fig. 2).

Since already at the unfired state sodium ions are enriched at the glass particle rim as a result of the glass integration within the alkaline milieu of the clay, it can be inferred that at these regions liquid phases are formed first. The regions identified as sodium-rich glass melt (Fig. 9) appear as darkly shaded areas which are imaged as reaction rims around the glass particles, too. Furthermore, sponge-like phases identified as Mg–Ca-silicates (diopside) can be recognised in the SEM.

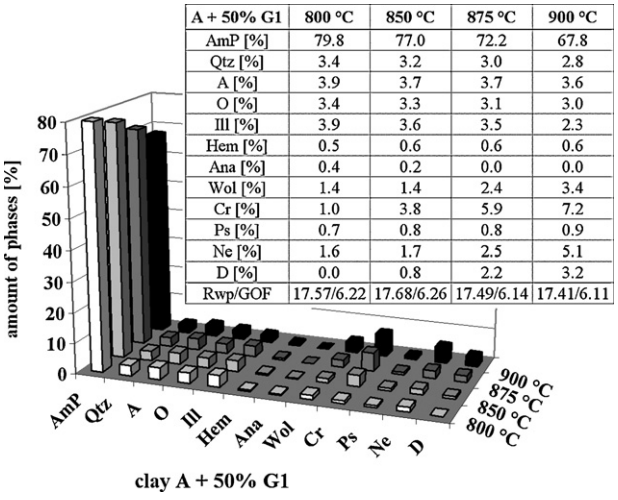

A + 50% G1	800 °C	850 °C	875 °C	900 °C
AmP [%]	79.8	77.0	72.2	67.8
Qtz [%]	3.4	3.2	3.0	2.8
A [%]	3.9	3.7	3.7	3.6
O [%]	3.4	3.3	3.1	3.0
Ill [%]	3.9	3.6	3.5	2.3
Hem [%]	0.5	0.6	0.6	0.6
Ana [%]	0.4	0.2	0.0	0.0
Wol [%]	1.4	1.4	2.4	3.4
Cr [%]	1.0	3.8	5.9	7.2
Ps [%]	0.7	0.8	0.8	0.9
Ne [%]	1.6	1.7	2.5	5.1
D [%]	0.0	0.8	2.2	3.2
Rwp/GOF	17.57/6.22	17.68/6.26	17.49/6.14	17.41/6.11

Fig. 5. Amounts of crystalline and amorphous phases due to 50% of alkali containing scrap glass powders G1 in clay A (XRD/Rietveld, standard: 20 wt.% CaF_2, refinement steps: preferred orientation (*h k l*): Qtz (0 1 0), Ill (1 −1 −1), Wol (0 0 2)).

A + 50% G2	800 °C	850 °C	900 °C
AmP [%]	80.1	74.1	66.3
Qtz [%]	3.3	3.3	2.9
A [%]	3.9	3.6	3.2
O [%]	3.3	3.2	2.8
Ill [%]	3.7	3.5	3.0
Hem [%]	0.5	0.6	0.6
Ana [%]	0.4	0.2	0.0
Wol [%]	1.3	1.4	2.6
Cr [%]	1.2	4.9	8.0
Ps [%]	0.6	0.7	0.9
Ne [%]	1.7	1.8	3.2
D [%]	0.0	2.7	6.5
Rwp/GOF	17.50/6.17	17.71/6.23	17.79/6.30

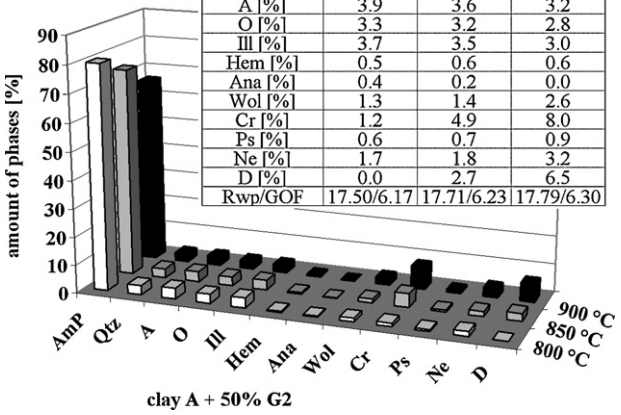

Fig. 6. Amounts of crystalline and amorphous phases due to 50% of alkali containing scrap glass powders G2 in clay A (XRD/Rietveld, standard: 20 wt.% CaF_2, refinement steps: preferred orientation (*h k l*): Qtz (0 1 0), Ill (1 −1 −1), Wol (0 0 2)).

A + 50% G4	800 °C	850 °C	875 °C	900 °C
AmP [%]	74.6	74.0	62.6	61.5
Qtz [%]	4.0	3.2	3.2	2.9
A [%]	3.9	1.8	2.8	2.6
O [%]	3.7	1.8	3.3	2.8
Ill [%]	3.9	3.7	2.8	2.3
Hem [%]	0.5	0.5	0.5	0.5
Ana [%]	0.6	0.3	0.0	0.0
Ne [%]	2.0	4.6	12.4	15.2
Cr [%]	1.4	2.4	2.7	2.7
Wol [%]	1.0	1.9	2.1	2.0
Ps [%]	0.6	0.8	0.8	0.9
En [%]	2.1	1.2	1.1	0.8
Ep [%]	1.3	1.3	1.1	1.2
D [%]	0.4	4.1	4.6	4.5
Rwp/GOF	17.81/6.2	17.40/6.0	16.36/5.7	15.38/5.4

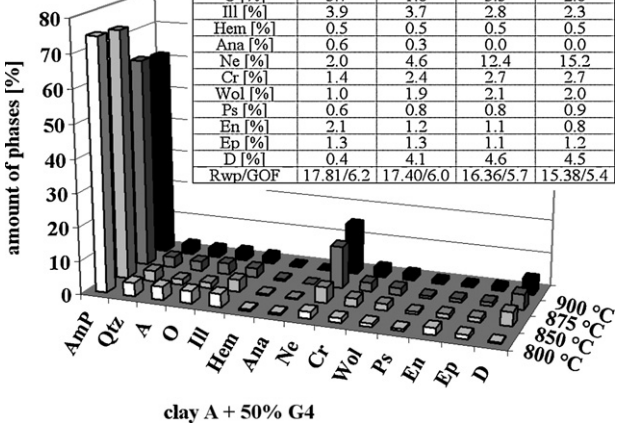

Fig. 7. Amounts of crystalline and amorphous phases due to 50% of alkali containing scrap glass powders G4 in clay A (XRD/Rietveld, standard: 20 wt.% CaF_2, refinement steps: preferred orientation (*h k l*): Qtz (0 1 0), A (0 0 2), O (0 0 2), Ill (1 −1 −1), Ep (0 0 4)).

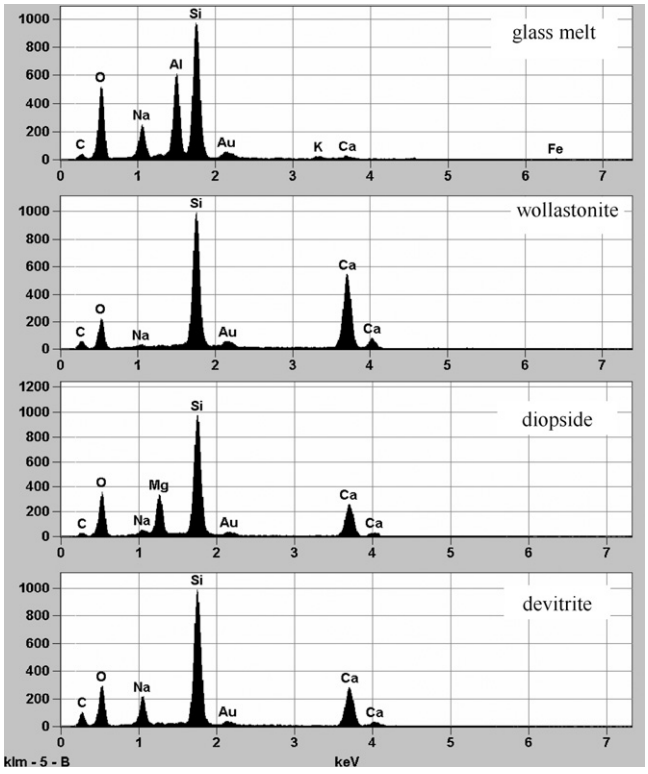

Fig. 9. EDS spectra of sodium-rich glass melt, wollastonite, diopside and devitrite of Fig. 8.

The light phase in Fig. 8 (right) was identified by EDX analysis as Na–Ca-silicate of the composition $Na_2O*3CaO*6SiO_2$ (devitrite) which had already been proven by Pontikes et al.[17] within glass containing ceramic bodies. However, since devitrite is described as needle- or brush-like after the current models[17–19], initially it was not sure whether devitrite is existent or not. By means of XRD no Na–Ca-silicate was found. However, completive investigations with higher amounts of scrap glass powders (60%) confirmed the formation of devitrite.

Furthermore, XRD investigations revealed that, although within the range of detection limit, enstatite and an epidot–similar phase are additionally formed due to the addition of G4 to clay A. This can be attributed to the higher amounts of

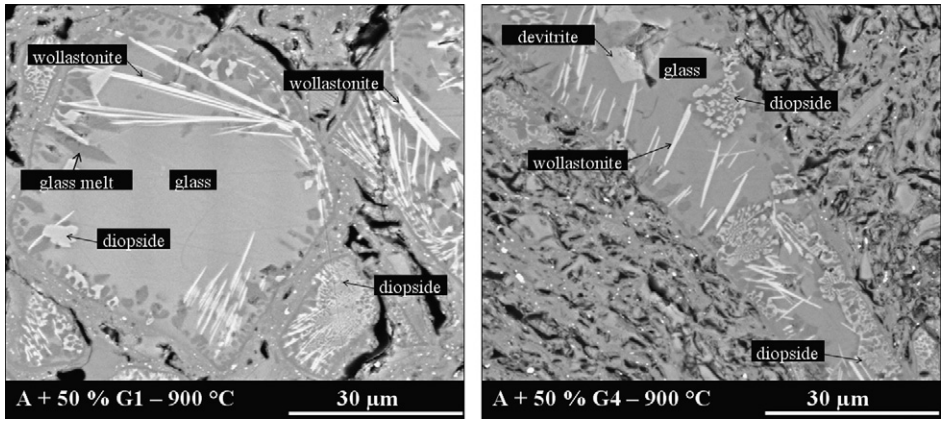

Fig. 8. Microstructure and secondary mineral phases due to the addition of glass powders to clay A (mix ratio clay:glass 1:1; left G1, right G4; firing temperature 900 °C, heating rate 2 K/min; SEM-BSE, 15 kV).

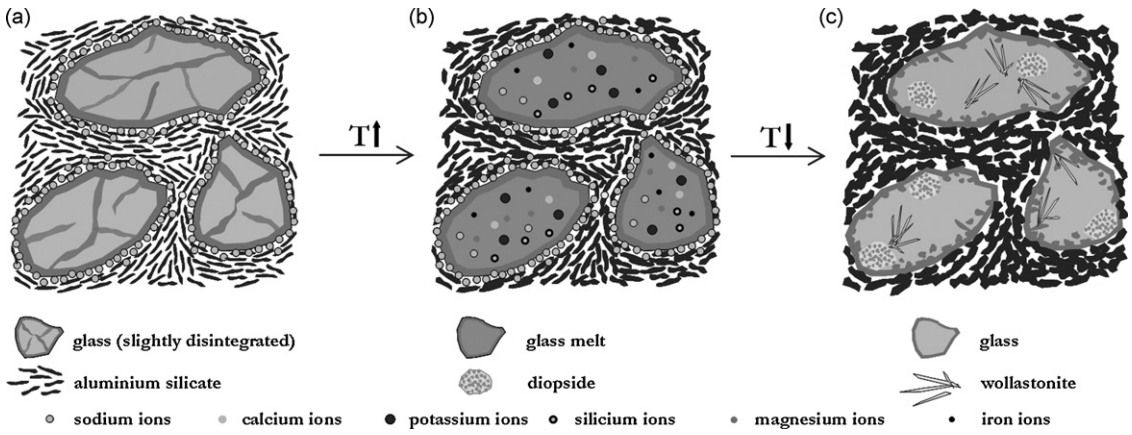

Fig. 10. Scheme of the mode of action of scrap glass powders within kaolinitic, carbonate-free clay A.

MgO and Fe_2O_3 within G4. Moreover, there is a lower formation of diopside within this batch (Fig. 4).

Initially, it seems to be contradictory that the highest amounts of nepheline are formed by the application of glass powder G4 which possesses the lowest Na_2O-content of the glass powders G1, G2 and G4 (Fig. 4). Nepheline is the only secondary mineral phase which binds Na_2O. Moreover, as there is a lower amount of cristobalite and at the same time an about equal amount of quartz it can be inferred that the formation of nepheline is preferred compared to the formation of cristobalite when a sufficient amount of Na_2O is present. As the glass powder G4 yields the highest amount of sodium ions when exposed to water (Table 3), it is further inferred that the mode of action of glass powders at the unfired state significantly affects the formation of mineral phases during firing and hence the body properties. This assumption is sustained by the fact that the formation of akermanite solely takes place after adding the finest borosilicate glass G3-3 which yields the highest amount of magnesium ions when exposed to water.

The proof of nepheline confirms the results of Pontikes et al.[17] who had detected nepheline when adding glass powders to clays poor in calcite. Furthermore, after Pontikes et al.[17] the impact of particle size distribution of the glasses consists in a faster sintering process with finer glass particles. However, the formation of new phases due to a higher grade of fineness of the glasses was not described by Pontikes et al.[17] The results presented within this paper augment current models by the proof that, in addition to the intensification of the sintering process, with a higher grade of fineness of the used glasses the formation of new phases, like e.g. akermanite due to G3-3 in clay A, is possible.

3.3. Material model

The basis for the sintering behaviour of the glasses is their dissolution by the alkaline environment within the clay. Depending on the chemical composition and the fineness of the scrap glass powders easily soluble alkalis and earth alkalis and in a further state silica anions are solubilised from the glass network. This process is impeded by the presence of increasing amounts of Al_2O_3 within the glass. Initially, the solution of sodium ions from the glass at the unfired state of the ceramic batch leads to an oriented agglomeration of clay minerals around the glass particles (Fig. 10a).[20,21]

With increasing firing temperatures above the transformation point of the glasses the glass particles within the kaolinitic, carbonate-free clay A are melted while, due to the high kaolinite content, the surrounding clay matrix undergoes no phase reactions indicating the sintering process up to high temperatures (Fig. 10b). Liquid phases are primarily formed at sodium-rich rims and cracks of the glass particles. According to the glass composition metal cations and silica anions are dissolved in the glass melt. Moreover, quartz is also disintegrated at the quartz–glass interface. Thereafter, with decreasing temperatures acicular wollastonite, cristobalite and diopside as well as minor phases crystallise (Fig. 10c).

The formation of nepheline takes place at the glass–kaolinite interface and depends on the predeterioration of the glass, i.e. on the concentration of dissolved sodium ions. By formation of nepheline the bond between glass particles and the surrounding matrix is obtained what contributes to the increase in body strength.

Dense sintered bodies can already be obtained at 900 °C depending on the chemical composition, the grade of preparation and the portion of glass. Within these dense bodies primary mineral phases of the clay (illite) and secondary mineral phases from the glass transformation (cristobalite) coexist. In contrast, secondary mineral phases like mullite and spinel typical for the sintering process of kaolinitic clays are not formed.

4. Conclusions

The phase reactions during the firing of traditional ceramic batches containing scrap glass powders are strongly influenced by chemical processes occurring within the unfired state. Depending on the particular composition and the fineness of the glasses a different mineralogy of the fired bodies was obtained. The occurring phase reactions are of significant influence on the body properties like shrinkage, strength and water absorption. The knowledge of occurring mineral phase (trans)-formations

can serve as basis for the confident assessment of product properties and resulting applications. Furthermore, inferences on resultant procedural impacts like alkali bursting or corrosion of the kiln equipment are possible. The latter cannot be assessed by solely determining the body properties without knowledge of occurring phase reactions.

Abbreviations

BET	Brunauer, Emmett, Teller
GOF	goodness of fit; measure of Rietveld refinement quality
R_{wp}	*R*-weighted pattern; measure of Rietveld refinement quality

Mineral phases

A	albite ($NaAlSi_3O_8$)
Ak	akermanite ($Ca_2MgSi_2O_7$)
AmP	amorphous phases [wt.%]
Ana	anatase (TiO_2)
Cr	cristobalite (SiO_2)
D	diopside ($CaMgSi_2O_6$)
En	enstatite ($MgSiO_3$)
Ep	epidote ($Ca_2Al_2Fe(SiO_4)_3OH$)
Fs	feldspar
Hem	hematite (Fe_2O_3)
Ill	illite ($KAl_2[Si_3AlO_{10}(OH)_2]$)
Kao	kaolinite ($Al_2(Si_2O_5)(OH)_4$)
Ms	muscovite ($KAl_2[(OH,F)_2\|AlSi_3O_{10}]$)
Mul	mullite ($Al_6Si_2O_{13}$)
Ne	nepheline ($(K,Na)AlSiO_4$)
O	orthoclase ($KAlSi_3O_8$)
Ps	pseudobrookite ((Fe_2TiO_5))
Qtz	quartz (SiO_2)
Sp	spinel ($MgAl_2O_4$)
Wol	wollastonite ($CaSiO_3$)

Acknowledgements

The present contribution resulted from extending the project Fundamental investigations on the influence of sintering aids on the sintering process of traditional ceramic microstructures[22] funded by the German Federation of Industrial Research Associations (AiF) at the F.A.-Finger-Institute for Building Materials Science (FIB), Bauhaus-University Weimar. Furthermore, we wish to thank the Federal State of Thuringia for the financial support awarded to A. Schwarz-Tatarin.

References

1. Schwarz A, Freyburg S. Interactions between sintering aids and clays within the sintering process of bricks. In: *Proceedings of the 10th International Conference and Exhibition of the European Ceramic Society*. 2007. p. 1743–50.
2. Schmidt E. *Die physikalischen und chemischen Veränderungen beim Ziegelbrand*. Institut für Ziegelforschung Essen e.V.; 1968.
3. Fischer P. Die Bildung des grobkeramischen Scherbens beim Brennen–2. Teil: Ausbildung des Scherbengefüges. *Ziegeleitechnisches Jahrbuch* 1987/1988:96–108.
4. Telle R, Brand. Chapter in: Salmang H, Scholze H, Keramik. 7. vollständig neubearbeitete und erweiterte Auflage. Hrsg. Telle R, Springer-Verlag, Berlin & Heidelberg; 2007.
5. Freyburg S, Baukeramisches Gefüge und Dauerhaftigkeit–Ein Beitrag zur Erhaltung historischer Ziegelmauerwerke. Dissertation, F.A. Finger-Institute for Building Materials Science, Bauhaus-University Weimar; 2004.
6. Bellotto M, Gualtieri A, Artioli G, Clark SM. Kinetic study of the kaolinite-mullite reaction sequence. Part I. Kaolinite dehydroxylation. *Physics and Chemistry of Minerals* 1995;**22**:207–14.
7. Gualtieri A, Bellotto M, Artioli G, Clark SM. Kinetic study of the kaolinite-mullite reaction sequence. Part II. Mullite formation. *Physics and Chemistry of Minerals* 1995;**22**:215–22.
8. Sadunas A, Giraitis R, Sveikauskaite A. Untersuchungen über den Einfluss zweiwertiger Ionen auf das Sintern. *Ziegelindustrie International* 1997;**3**:127–39.
9. Chesters JH. *Refractories–production and properties*. London: The Iron and Steel Institute; 1973, ISBN 0 900497 84 X.
10. Krause E, Berger I, Kröckel O, Maier P. Technologie der Keramik. In: *Band 3–Thermische Prozesse.* Berlin: Verlag für Bauwesen; 1982.
11. Jasmund K, Lagaly G. *Tonminerale und Tone – Struktur, Eigenschaften, Anwendung und Einsatz in Industrie und Umwelt*. Darmstadt: Steinkopff Verlag; 1993.
12. Moore DM, Reynolds RC. *X-ray diffraction and the identification and analysis of clay minerals*. Oxford (NY): Oxford university Press; 1989.
13. Meier L, Kahr G. Determination of the cation exchange capacity (CEC) of clay minerals using the complexes of copper(II) ion with triethylenetetramine and tetraethylenepentamine. *Clays and Clay Minerals* 1999;**47**(3):386–8.
14. Bundesverband Glasindustrie e.V./Fachvereinigung Behälterglasindustrie e.V.; 2008. http://www.glasaktuell.de.
15. Schwarz-Tatarin A, Wirkmechanismen anorganischer Sekundärrohstoffe in silicatkeramischen Massen, PhD Thesis, F.A. Finger-Institute for Building Materials Science, Bauhaus-University Weimar, ISBN: 978-3-86727-978-9, Göttingen: Cuvillier; 2009.
16. La Course WC, Mason W. Glaze problems from a glass science perspective. In: Henkes VE, Onoda GY, Carty WM, editors. *Science of whitewares*. Westerville, Ohio: American Ceramic Society; 1995. p. 339–56.
17. Pontikes Y, Esposito L, Tucci A, Angelopoulos GN. Thermal behaviour of clays for traditional ceramics with soda-lime-silica waste glass admixture. *Journal of the European Ceramic Society* 2007;**27**:1657–63.
18. Scholze H, Glas: Natur. *Struktur und Eigenschaften 3. Neubearb. Auflage*. Berlin u.a: Springer Verlag; 1988.
19. Vogel W. *Glaschemie. 3. völlig überarb. und aktual. Auflage*. Berlin u.a: Springer Verlag; 1988.
[20]. Williamson WO, Strength and Microstructure of Dried Clay Mixtures, Ceramic Processing before Firing, ed. Onoda G.Y., Hench L.L., 1978, 379–386.
21. Anderson S, Tandon D, Kohlenberger LB, Blair FG. Strength of adhesion of dried clay slurries to window glass as a function of slurry pH. *Journal of American Ceramic Society* 1969;**52**:521.
22. Freyburg S, Bettzieche H, Schwarz A. *Final report "Grundlegende Untersuchungen zur Beeinflussung der Stoffbildungsprozesse baukeramischer Gefüge durch den Einsatz von Sinterhilfsmitteln (SHM)" Fo.-A.-Nr.: AiF 13442/BR.*. Weimar: F.A. Finger-Institute for Building Materials Science, Bauhaus University; 2005.